Computational Predictions on the Receptive Fields and Organization of V2 for Shape Processing

Yiu Fai Sit and Risto Miikkulainen
Department of Computer Sciences
The University of Texas at Austin
Austin, TX 78712, U.S.A.
{yfsit, risto}@cs.utexas.edu

Abstract

It has been more than 40 years since the first studies of the secondary visual cortex (V2) were published. However, no concrete hypothesis on how the receptive field of V2 neurons support general shape processing has been proposed to date. Using a computational model that follows the principle of self-organization, two hypotheses are advanced in this paper: (1) A typical V2 orientation-selective receptive field contains a primary orientation and a secondary orientation component, forming a corner, a junction, or a cross; (2) V2 columns with the same primary orientation form contiguous domains, divided into subdomains that prefer different secondary orientations. The first hypothesis is consistent with existing experimental evidence, and both hypotheses can be tested with current techniques in animals. In this manner, computational modeling can be used to provide verifiable predictions that eventually allow us to understand the role of V2 in visual processing.

1 Introduction

Representation of shape in the cortex is generally believed to be hierarchical (Felleman & Van Essen, 1991). At the bottom lies the primary visual cortex (V1), which is the largest visual area and relatively well understood (Hubel & Wiesel, 1959, 1962). V1 acts primarily as a local feature detector. As information travels up in the hierarchy, receptive fields get larger and more complicated, and finally, in areas like IT, neurons are selective to objects.

The major second stage of processing after V1 is the secondary visual cortex (V2), which is only slightly smaller than V1 and located next to it in the cortex (Weller & Kaas, 1983; Felleman & Van Essen, 1991). Studies of V2 have a long history (Hubel & Wiesel, 1965), beginning at about the same time as those of V1. Despite this history, the receptive field properties of V2 neurons are largely unknown (Boynton & Hegdé, 2004).

Previous studies tried to address this question by using a set of artificial stimuli like contours, angles, and circular patterns (Hegdé & Van Essen, 2000, 2003; Ito & Komatsu, 2004; Mahon & de Valois, 2001). These studies showed that V2 neurons are selective to some of the patterns over the others in the set. However, only limited conclusions can be drawn from such studies. The underlying preferred visual patterns of the V2 neurons can be different from the set of stimuli used and it is difficult to find out if this is the case. Reverse correlation methods based on single stage linear-nonlinear model of spike generation have been successful in mapping the receptive fields in V1 (Jones & Palmer, 1987; DeAngelis, Ohzawa, & Freeman,

1993; Ringach, 2004), but it is difficult to extend this model to multiple stages in order to study higher level visual areas (Schwartz, Pillow, Rust, & Simoncelli, 2006). It is therefore difficult to determine the receptive field properties by physiological methods alone.

The approach taken in this paper is to use a computational model with realistic constraints and natural images as inputs to obtain verifiable predictions on the receptive field properties and organization of form perception in V2. The main advantage of the computational approach over previous studies is that the receptive fields can be directly determined from the afferent connections from V1. The model used in this study is based on the LISSOM architecture (Laterally Interconnected Synergetically Self-Organizing Map; Miikkulainen, Bednar, Choe, & Sirosh, 2005; Sirosh & Miikkulainen, 1994), which has been used extensively to understand how the organization of V1 emerges during development through input-driven self-organization. Extended to include V2, LISSOM developed realistic properties in both the model V1 and V2, providing a foundation for predicting the receptive fields and organization in V2.

The LISSOM model predicts that a typical V2 receptive field contains a primary orientation and a secondary orientation component, forming a corner, a junction, or a cross, depending on their relative locations. Results from two independent physiological studies (Anzai & Van Essen, 2001, 2002; Anzai, Van Essen, Peng, & Hegdé, 2002; Ito & Komatsu, 2004) are consistent with this prediction. The model also predicts that cortical columns that prefer the same primary orientation form contiguous domains in V2. Each orientation domain is divided into subdomains that prefer different secondary orientations. These subdomains may span all orientations, making each V2 orientation domain similar to the orientation hypercolumn in V1. Both predictions can be verified in future physiological experiments using existing techniques. This research thus demonstrates how computational modeling can be used to provide insights that eventually lead to deeper understanding of visual processing in the brain.

2 Related Work

Previous computational models of V2 usually have hand-designed receptive fields and lateral connections that are specific to the biological experiments being modeled. For example, to model contour integration and perceptual grouping, receptive fields of collinear (Ross, Grossberg, & Mingolla, 2000) or curved lines (wide corners; Neumann & Sepp, 1999) are used. In addition, a Gaussian weight profile can be used for the V1-V2 projections to model surround suppression (Sullivan & de Sa, 2006). To explain why the response to the same local edge depends on whether it belongs to the border of foreground or background, (i.e. border ownership; Zhou, Friedman, & von der Heydt, 2000), a sophisticated lateral connection pattern can be constructed. Each neuron excites those neurons that encode consistent border segments and inhibits those that encode inconsistent ones (Zhaoping, 2005).

In some of these models the V2 receptive fields are learned from the inputs. However, the training patterns are artificially constructed with a particular task in mind, e.g. they consist of corners (Taylor, Hartley, & Taylor, 2005; Sit & Miikkulainen, 2006), rectangles (Grossberg & Williamson, 2001), letters (Deco & Rolls, 2004), or single objects (Plebe, 2007).

While these models can explain a specific phenomenon, it is unclear how such specific connectivity can arise in the cortex through visual experience, and whether it can support shape processing in general. In this paper, natural images are used to train a joint V1 and V2 model with initially random connection weights. After self-organization, the receptive fields and lateral connections reflect the statistics of natural images, suggesting a biologically-plausible hypothesis on how the specific receptive fields and lateral connection patterns can arise. Furthermore, they are constructed based on correlations in the input, not by demands of any particular visual task, suggesting that they support shape processing in general.

3 Computational Model

The computational model is based on the LISSOM architecture (Laterally Interconnected Synergetically Self-Organizing Map; Miikkulainen et al., 2005; Sirosh & Miikkulainen, 1994), extended to include a neural sheet for V2. LISSOM has been used extensively to understand how the organization of the primary visual cortex emerges through self-organization during development. In this section, the model's architecture, activation functions of the units, and their learning rules are described.

3.1 Architecture of the Model

In LISSOM, cortical visual areas are two-dimensional sheets of units representing vertical columns of cells through the six layers of the biological cortex. Each unit receives input from lower level units, as well as lateral input from the units on the same sheet (Figure 1).

In the extended model, each V2 unit receives afferent input from V1 units, which in turn receive input from two types of neurons in the LGN: ON-center and OFF-center. The LGN units receive input from a small area of the retina, represented as an array of photoreceptor units. For simplicity, the ON and OFF LGN channels are represented as two separate sheets. In addition to the excitatory afferent connections, each cortical unit has reciprocal excitatory and inhibitory lateral connections with other units.

The long-range lateral connections are inhibitory in LISSOM, for two reasons. First, they model biological lateral interactions with high-contrast inputs, i.e. inputs that have the strongest effect on self-organization. Using high-contrast gratings of different sizes, Sceniak, Hawken, and Shapley (2001) found that the surround influences tend to be excitatory locally but inhibitory at longer ranges in macaque V1. Inhibition from surrounding line segments that have the same orientation as the center has also been observed in monkey (Knierim & van Essen, 1992). Similar effects are seen in vitro in ferret (Weliky, Kandler, Fitzpatrick, & Katz, 1995) and in cat (Hirsch & Gilbert, 1991) as well. Therefore, although most of the lateral connections in the cortex are excitatory, inhibition seems to dominate under high-contrast input. Such an effect is likely to be due to inhibitory interneurons that have high thresholds (Weliky et al., 1995; Angelucci et al., 2002; Miikkulainen et al., 2005). This circuitry can be approximated by inhibitory long-range connections, as is done in LISSOM. Second, long-range inhibition provides a local computational mechanism for competition, which is essential for proper self-organization. The long-range inhibitory connections are therefore both physiologically and computationally essential in order to model self-organization effectively.

3.2 Photoreceptor and LGN Activation

A single model photoreceptor is represented by a pixel in the input image. Since this study focuses on shape processing, the current model is achromatic. The activation of the model photoreceptors therefore consists of pixel values of gray-scale input images.

The connections from the model retina to the LGN units are fixed and chosen to approximate the receptive fields that have been measured in adult LGN cells, using a standard difference-of-Gaussians model (Cai, DeAngelis, & Freeman, 1997; Rodieck, 1965; Tavazoie & Reid, 2000). First, the center of each LGN receptive field is mapped to the location in the retina corresponding to the location of the LGN unit. This mapping ensures that the LGN will have the same two-dimensional topographic organization as the retina. Using that location as the center, the weights are then calculated from the difference of two normalized Gaussians. More precisely, the weight $L_{xy,ab}$ from photoreceptor (x, y) in the receptive field of an ON-center unit (a, b) with center (x_c, y_c) is given by

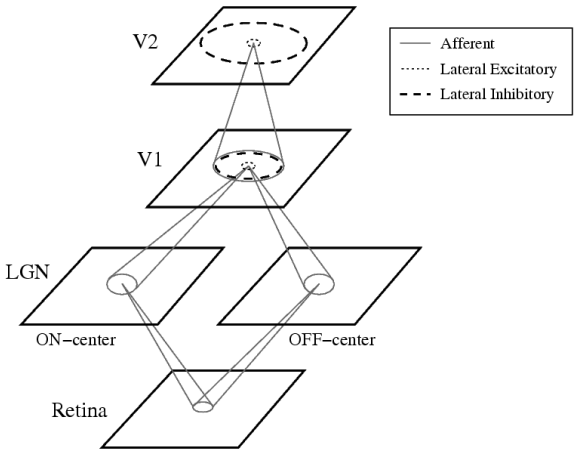

Figure 1: **Architecture of the extended LISSOM model.** The model is a hierarchy of sheets of neural units that represent the retina, ON and OFF channels in LGN, V1, and V2. Sample connections are indicated for one unit in the LGN channels and the model cortical areas. The LGN afferents form a local anatomical receptive field on the retina. Neighboring LGN units have different but overlapping receptive fields. Similarly, V1 units have afferent projections from the LGN sheets, and V2 units receive local input from units in V1. The afferent projections increase in size (not drawn to scale) at each level. V1 and V2 units also have short-range lateral excitatory (dotted circle) and long-range lateral inhibitory (dashed circle) connections. The receptive fields and long-range lateral connections in V2 are about twice as large as those in V1, similar to those measured in monkey cortex (Amir et al., 1993).

$$L_{xy,ab} = \frac{\exp\left(-\frac{(x-x_c)^2+(y-y_c)^2}{\sigma_c^2}\right)}{\sum_{uv}\exp\left(-\frac{(u-x_c)^2+(v-y_c)^2}{\sigma_c^2}\right)} - \frac{\exp\left(-\frac{(x-x_c)^2+(y-y_c)^2}{\sigma_s^2}\right)}{\sum_{uv}\exp\left(-\frac{(u-x_c)^2+(v-y_c)^2}{\sigma_s^2}\right)},$$

where σ_c determines the width of the central Gaussian and σ_s the width of the surround Gaussian. The weights for an OFF-center unit are the negative of the ON-center weights.

The units in the ON and OFF channels of the LGN compute their responses as a squashed weighted sum of activity in their receptive fields. More precisely, the response ξ_{ab} of ON or OFF-center unit (a,b) is calculated as

$$\xi_{ab} = \sigma\left(\sum_{xy}\chi_{xy}L_{xy,ab}\right),$$

where χ_{xy} is the activation of model photoreceptor (x,y) in the receptive field of (a,b), $L_{xy,ab}$ is the afferent weight from (x,y) to (a,b), and σ is a piecewise linear sigmoid activation function.

3.3 Cortical Activation

The cortical activation mechanism is similar to that of the LGN, but extended to include lateral interactions. The total activation is computed by combining the afferent and lateral contributions. First, the afferent stimulation s_{1ij} of V1 unit (i,j) is calculated as a weighted sum of activations in its receptive fields on the LGN:

$$s_{1ij} = \gamma_A \left(\sum_{ab \in ON} \xi_{ab} A_{1ab,ij} + \sum_{ab \in OFF} \xi_{ab} A_{1ab,ij} \right),$$

where ξ_{ab} is the activation of neuron (a,b) in the receptive field of V1 unit (i,j) in the ON or OFF channels, $A_{1ab,ij}$ is the corresponding afferent weight, and γ_A is a constant scaling factor. Variables that are specific to V1 are indicated with the subscript 1, and those specific to V2 with subscript 2. The initial response or firing rate of unit (i,j) is

$$\eta_{1ij}(0) = \sigma(s_{1ij}).$$

After the initial activation, V1 activity settles through short-range excitatory and long-range inhibitory lateral interactions:

$$\eta_{1ij}(t) = \sigma \left(s_{1ij} + \gamma_E \sum_{kl} \eta_{1kl}(t-1) E_{1kl,ij} - \gamma_I \sum_{kl} \eta_{1kl}(t-1) I_{1kl,ij} \right),$$

where $\eta_{1kl}(t-1)$ is the activity of another V1 unit (k,l) during the previous time step, $E_{1kl,ij}$ is the weight of the excitatory lateral connection from that unit to unit (i,j), and $I_{1kl,ij}$ is the inhibitory connection weight. All connection weights have positive values. The scaling factors γ_E and γ_I represent the relative strengths of excitatory and inhibitory lateral interactions of the model.

For simplicity, V2 is activated after the response in V1 has settled, at time step t'. Similarly to V1, the activation η_{2mn} of V2 unit (m,n) is defined as a sum of afferent and lateral contributions:

$$\eta_{2mn}(t) = \sigma \left(\gamma_A \sum_{kl} \eta_{1kl}(t') A_{2kl,mn} + \gamma_E \sum_{pq} \eta_{2pq}(t-1) E_{2pq,mn} - \gamma_I \sum_{pq} \eta_{2pq}(t-1) I_{2pq,mn} \right),$$

where $\eta_{1kl}(t')$ is the settled response of the V1 unit (k,l), $A_{2kl,mn}$ is the corresponding afferent weight, and $E_{2pq,mn}$ and $I_{2pq,mn}$ the excitatory and inhibitory lateral connection weights from V2 unit (p,q) to unit (m,n).

3.4 Learning

After the activity has settled, the connection weights of each cortical unit are modified. All the afferent and lateral weights adapt according to the same biologically motivated mechanism: the Hebb rule (Hebb, 1949) with divisive postsynaptic normalization:

$$w'_{xy,ij} = \frac{w_{xy,ij} + \alpha X_{xy} \eta_{kij}}{\sum_{uv} (w_{uv,ij} + \alpha X_{uv} \eta_{kij})},$$

where $w_{xy,ij}$ is the current afferent or lateral connection weight (either A_k, E_k, or I_k, $k = 1,2$) from (x,y) to (i,j), $w'_{xy,ij}$ is the new weight, α is the learning rate for each type of connection (α_A for afferent weights, α_E for excitatory, and α_I for inhibitory), X_{xy} is the presynaptic activity after settling (ξ for afferent in V1, η_1 for afferent in V2, η_1 for lateral in V1, and η_2 for lateral in V2), and η_{kij} stands for the activity of unit (i,j) of visual area Vk after settling. Afferent inputs (in V1, both ON and OFF channels together), lateral excitatory inputs, and lateral inhibitory inputs of each unit are normalized separately.

Normalization prevents the weight values from increasing without bounds; this process corresponds to redistributing the weights so that the sum of each weight type for each neuron remains constant. Such normalization can be seen as an abstraction of neuronal regulatory processes (Bourgeois, Jastreboff, & Rakic, 1989; Hayes & Meyer, 1988a, 1988b; Murray, Sharma, & Edwards, 1982; Pallas & Finlay, 1991; Purves, 1988; Purves & Lichtman, 1985; Turrigiano, 1999). Normalization, however, does not prevent single connections from dominating and effectively becoming the sole input to a unit. On the other hand, a cortical neuron receives input from hundreds to thousands of other neurons. It is also very unlikely that the inputs from a few neurons can completely determine the activity of a neuron. To enforce such a constraint in the model, a parameter w_{lim} is defined to limit the maximum attainable weight of individual cortical connections. When a weight exceeds w_{lim} after normalization, it is set to w_{lim} and the residue is distributed evenly to all the other connections so that the total weight remains constant. In other words, $1/w_{\text{lim}}$ is the minimum number of active connections within a receptive field; this parameter prevents the receptive fields from converging to an unrealistically low number of connections.

4 Simulations

The model was instantiated with parameter values constrained by biological data to simulate the development of monkey V1 and V2. At each simulation iteration, natural images were presented on the model retina, which resulted in the activation of the LGN, V1, and V2. The connection weights of the cortical units were then adjusted according to the Hebb rule as described in the previous section. As a result, the cortical units learned correlations in their inputs that were based on the statistics of natural images.

The sizes of the model areas and the extent of their connections are based on those in macaque monkey at about 5° eccentricity. The model retina has 48×48 pixels, representing a visual area of about 4°. In the LGN, the widths of the center (σ_c) and surround (σ_s) Gaussians are 0.5 and 2.0, respectively. There are 192×192 units in both the model V1 and V2. The receptive field radius of V1 is 5.5 units on the LGN, corresponding to about 1° visual field. At 5° eccentricity, the lateral connections in V1 are about twice as wide as the receptive fields (Angelucci et al., 2002), i.e. have a 44-unit radius. In the cortex, their average radius is about 3mm (Angelucci et al., 2002), therefore 15 units in the model V1 and V2 correspond to about 1mm in the biological cortex. The two model cortical areas therefore correspond to about 13×13mm.

The receptive fields of V2 are about twice as large as those in V1 (Gattass, Gross, & Sandell, 1981; Burkhalter & Van Essen, 1986), so the receptive field radius of a V2 unit is 44. The lateral connections in V2 are about twice as long as in V1 (Amir et al., 1993), hence the radius of the long-range inhibitory connections is 88 units. In both V1 and V2, the short-range excitatory connections have a radius of 1.5.

All weights are initialized randomly according to uniform distribution. The scaling factors for afferent and excitatory lateral connections, γ_A and γ_E, are both 1, and $\gamma_I = 2.5$ for inhibitory lateral connections. Small changes to these values yield roughly equivalent results. The number of time steps, t', that V1 response stabilizes is found to be less than 9. The individual cortical afferent and inhibitory connection weights are limited with $w_{\text{lim}} = 0.004$; any value between 0.01 and 0.001 produces similar results.

The inputs consist of 13 images arbitrarily selected from a collection of natural scenes (Hateren & Schaaf, 1998; Figure 2). Each of these images contains 768×576 pixels. At each training iteration, a 48×48 region is selected randomly from one of the images and presented to the retina. The simulation was run for $50,000$ iterations, at which point self-organization had reached a dynamic equilibrium.

Figure 2: **The set of images used in the simulation.** These images were randomly chosen from the still image collection of Hateren and Schaaf (1998). Each image has 768×576 pixels; regions of 48×48 pixels were randomly selected from them to train the model. Such images represent the variety of features normally found in natural environment.

5 Results

Given the parameterization of the model, at the end of the simulation, the model is intended to represent the cortical organization of an adult monkey. In this section, the orientation column structure, lateral connectivity, and receptive field properties of the model V1 and V2 are analyzed and compared with those in monkeys. Predictions are developed for future biological experiments in the next section.

5.1 Results in V1

In order for the V2 results to be meaningful, the model V1 must present biologically realistic input to it. The model V1 orientation map, lateral connections, and receptive field properties are analyzed in this section and verified with data from the macaque.

Figure 3 compares orientation maps from the model and macaque monkey, drawn to scale. The match is very good: The sizes, shapes, and spacing of the orientation domains are similar, and both maps contain the typical features found in animal maps, such as pinwheels and linear zones (Blasdel, 1992).

Figure 4 shows the afferent connections from the LGN, and the short-range excitatory and the long-range inhibitory connections of four sample V1 units. The long-range lateral connections form patchy clusters and mostly link units of similar orientation preference. More precisely, for the central 400 units in the model V1, each separated by four units from its neighbors, $65\% \pm 5\%$ of the lateral connections link similar $(\pm 45^\circ)$

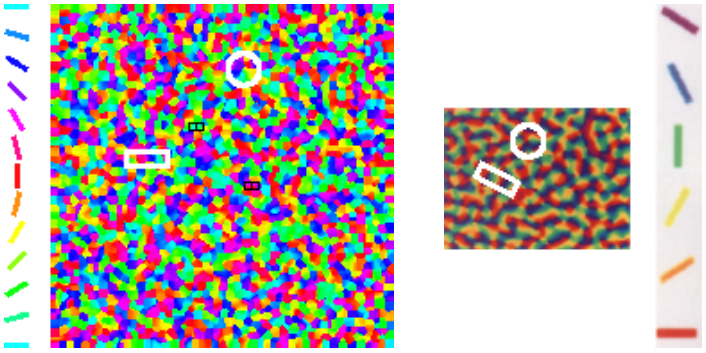

(a) (b)

Figure 3: **Orientation maps in the model V1 and in the macaque monkey (color figure).** (a) The orientation map of the model V1 after self-organization. This map corresponds to a 13×13mm area of the cortex. Orientations are color-coded, as shown on the left; the same coding will be used throughout the paper. Neighboring units often prefer similar orientations, forming clusters on the map. The white circles and the rectangle identify an example pinwheel and a linear zone, respectively. The small black squares located between the pinwheel and the linear zone indicate the locations of the V1 units shown in Figure 4. (b) The orientation map of a macaque monkey over a 7×5mm region (Blasdel, 1992). Its scale is the same as in (a) and a sample pinwheel and a linear zone are indicated. The color coding is different and is shown on the right. The two maps have similar structures, suggesting the model V1 can be used as a realistic input for self-organizing the model V2.

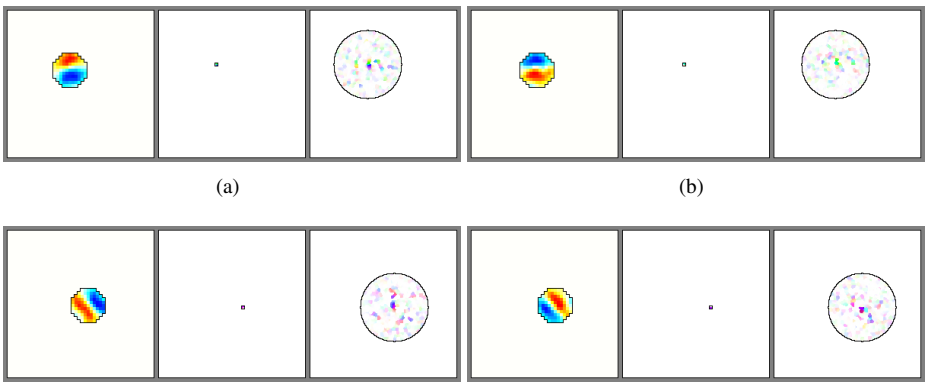

(a) (b)

(c) (d)

Figure 4: **Connections of four sample V1 units (color figure).** In each panel (from left to right), the afferent, lateral excitatory, and lateral inhibitory connections of one of the units indicated by a black square in Figure 3a are shown. Blue and orange in the afferent connections correspond to ON and OFF LGN cells, respectively. For lateral connections, the same color code is used as in the orientation map (Figure 3a) to indicate the orientation preference of the source unit. Connection strength is coded by intensity. (a) A V1 unit that prefers horizontal edges. (b) A V1 unit adjacent to (a), which also prefers horizontal edges at the same visual field, but with a different phase. (c,d) Another pair of adjacent V1 units: These units prefer a 135° orientation at different phases. The long-range lateral connections in these units are patchy, linking units of similar orientation preference that are aligned to the unit's preferred orientation. These results are consistent with biological data (Malach et al., 1993; DeAngelis et al., 1999).

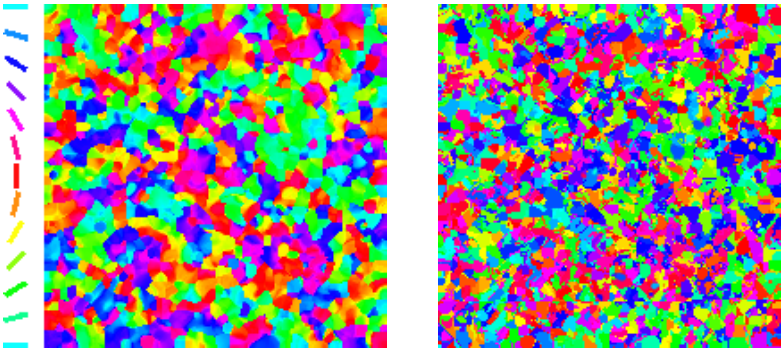

(a) (b)

Figure 5: **The orientation map and secondary orientation preferences in the model V2 (color figure).** (a) The orientation map of V2. In contrast to the smoothly changing orientation preferences in V1, the orientation preference often changes abruptly and discontinuously in V2. The orientation domains are also larger than those in V1. These two characteristics are consistent with measurements in the macaque (Hubel & Livingstone, 1987; Malach et al., 1994; Lu & Roe, 2007). (b) The secondary orientation preference of each V2 unit. Units that have the same preference form small clusters. Within a single orientation domain, there are usually several such clusters. The LISSOM model therefore predicts that each orientation domain is a hypercolumn that contains different secondary orientations.

orientation domains. In macaque V1, lateral connections are also patchy (Livingstone & Hubel, 1984), and $70\% \pm 10\%$ of them link cells located in similar $(\pm 45^\circ)$ orientation domains (Malach et al., 1993). The model V1 therefore has realistic lateral connection patterns.

Most of the V1 units are orientation-selective; those that are not (about 1%) are located primarily near pinwheels and fractures. Adjacent V1 units that prefer similar orientations are often selective for different phases (e.g. Figures 4a and 4b). Similarly, in the macaque, adjacent V1 cells of similar orientation preference are found to be selective for different phases in the same visual space (DeAngelis et al., 1999; D. A. Pollen & Ronner, 1981; Liu, Gaska, Jacobson, & Pollen, 1992). The model V1 therefore has realistic receptive field organization.

Such a good agreement between the model and biological data suggests that the model V1 can provide realistic input to the model V2 area.

5.2 Results in V2

In this section, the orientation map, the lateral connectivity, and the response properties of the model V2 are analyzed and compared with biological data.

The orientation preference map of the model V2 plots, for each unit, the orientation of the full-field sinusoidal grating that elicits the largest response from that unit (Figure 5a). Similar to the model V1, most V2 units are orientation-selective and neighboring units often have similar receptive fields. The orientation domains, however, are larger than those in V1, with abrupt changes of the preferred orientation. These results agree with the findings so far (Hubel & Livingstone, 1987; Malach et al., 1994; Lu & Roe, 2007).

The long-range lateral connections of V2 units are patchy, with patches slightly bigger and their separation wider than in V1 (Figure 6). These connections link units with similar orientation preference more frequently than those with very different orientations. For the 400 units at the center, 58% of these connections target units of similar $(\pm 30^\circ)$ primary orientation preference. In macaque V2, the lateral connections

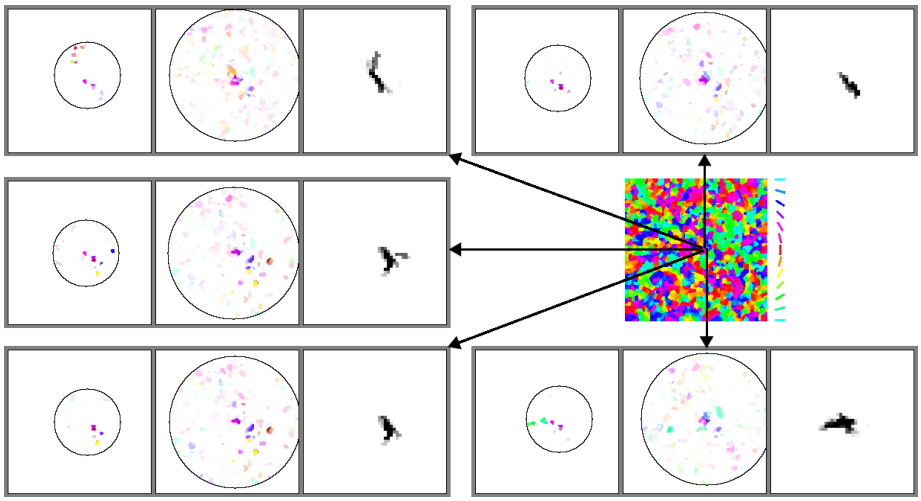

(a)

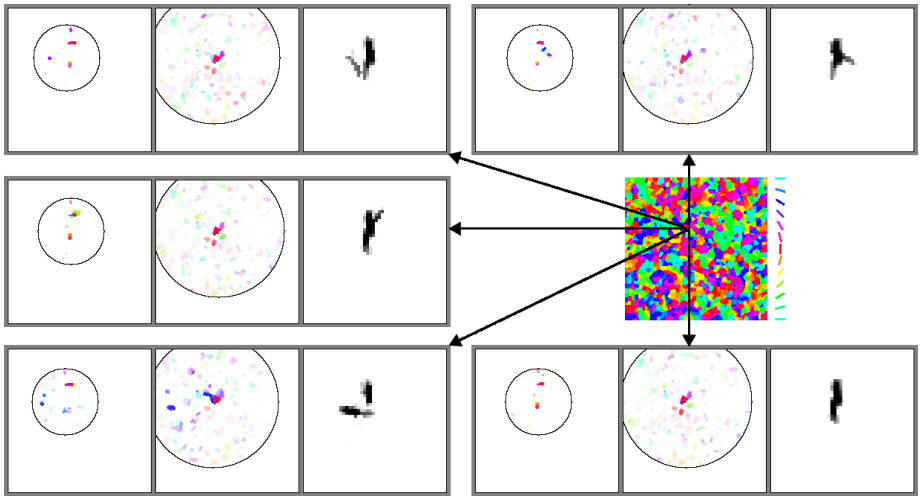

(b)

Figure 6: **Connections and preferred patterns of V2 units in the same orientation domain (color figure).** Each panel shows (from left to right) the afferent connections from V1, the inhibitory lateral connections from V2, and the preferred pattern on the retina for one V2 unit. The preferred pattern is computed by the weighted sum of the stimuli that maximally excite the V1 units with non-zero weights (as shown in the left panel). These stimuli are determined separately for each V1 unit by fitting a line segment to the unit's receptive field. For example, each of the V2 units in (a) receive strong afferent connections from a V1 unit slightly to the right and below the center of V1. The receptive field of that unit is displayed in the left panel of Figure 4d, showing that its preferred pattern is a line segment of about 135°. As a result, all the V2 units shown in (a) belong to the same orientation domain that prefers about 135°. Arrows indicate where each of these units are in V2. At different locations within the orientation domain, in addition to the primary orientation, a unit can also have a different secondary orientation within its receptive field. The top left, bottom left, and bottom right units have a near vertical, 45°, and horizontal secondary orientation preferences at different locations, forming a corner, a junction, and a cross, respectively. There are also some less common cases: The middle left unit has an extra third orientation preference and the top right unit does not have a secondary orientation preference at all. (b) V2 units within a different orientation domain, showing a similar structure of secondary orientation preferences. The afferent and lateral connectivity patterns match those found in monkeys (Malach et al., 1994; Anzai & Van Essen, 2001, 2002; Anzai et al., 2002). The preferred patterns (corner, junction, and cross) and the existence of substructures within V2 orientation domain are predictions of the LISSOM model.

are patchy as well. These patches are about as large in V1 and in V2, while their separation is wider in V2 (Malach et al., 1994). Lateral connections in macaque V2 also tend to link patches with similar orientation preference. More precisely, 50.3% of the lateral connections studied by Malach et al. (1994) link domains of similar ($\pm 30^\circ$) orientations. The results of the model V2 are therefore consistent with these data.

As in V1, such lateral connectivity may help in the grouping of contours. The larger receptive field and longer lateral connections in V2 may result in groupings of bigger components, rather than short line segments as in V1, to form simple shapes or borders between objects (Zhou et al., 2000).

To compare the response properties of the model with physiological studies of V2, the set of 128 gratings and contours used by Hegdé and Van Essen (2000, 2003) were presented to the receptive fields of the 400 units located at the center of V2. Selectivity index, defined as $1 - (R_{avg}/R_{max})$, where R_{avg} is the average response to all the stimuli and R_{max} is the response to the most effective stimulus, of these V2 units had an average of 0.8, which is similar to the value of 0.69 found by Hegdé and Van Essen (2003). A major finding of Hegdé and Van Essen (2003) was that 84% of the V2 cells have a higher selectivity for contours than gratings, although the average response is significantly larger for contours than gratings in only 24% of the cells. These results are also comparable in our model: 70% of the V2 units are more selective for contours, while 39% of the units have a larger average response to contours than gratings.

In a related study based on the same set of stimuli (Hegdé & Van Essen, 2000), 39% of the V2 cells responded better to sinusoidal gratings than to hyperbolic, concentric, and radial gratings. Among the different contours, bar and acute angle ($\approx 45^\circ$) were the best stimuli for 16% and 17% of the cells, respectively. The model V2 has similar preferences: 52% of the units prefer sinusoidal gratings to other types of gratings, while 23% prefer the bar, and 29% prefer the acute angle. In a similar study, Ito and Komatsu (2004) measured the response of V2 cells to corners of different angles and orientations. The proportion of the cells that preferred sharp angle (30°), wide angle ($60^\circ - 150^\circ$), and straight bar were 43.1%, 40.5%, and 16.3%, respectively. The model has a similar distribution: 34%, 47%, and 19%.

The properties of the model V1 and V2 after self-organization are therefore consistent with biological data, suggesting the model is a valid representation of these two cortical areas. The model can then be analyzed in more detail to gain insight into properties that have not yet been studied experimentally, as will be done next.

6 Predictions of the Model

In this section, predictions of the model on the preferred visual patterns and organization within the orientation domains of V2 are discussed.

6.1 Preferred Visual Patterns of V2

Each model V2 unit receives strong input from a group of V1 units that have the same orientation preference as that V2 unit (Figure 6). In addition, many V2 units also receive an extra but weaker secondary orientation input from V1 at a subregion within the receptive field, which may overlap the primary orientation in visual space. A typical model V2 receptive field therefore contains two orientation components with different strengths.

As shown in Figure 6, it is possible to predict the preferred visual pattern of a V2 unit based on the patterns that maximally excite the afferent V1 units and the associated connection weights. The preferred patterns for 100 sample V2 units were obtained this way and shown in Figure 7. To illustrate the variety of preferred stimuli, each unit in the figure is located 10 units apart (which corresponds to a separation of about 0.7mm in the cortex) in the central area of the V2 network. The patterns have different orientations

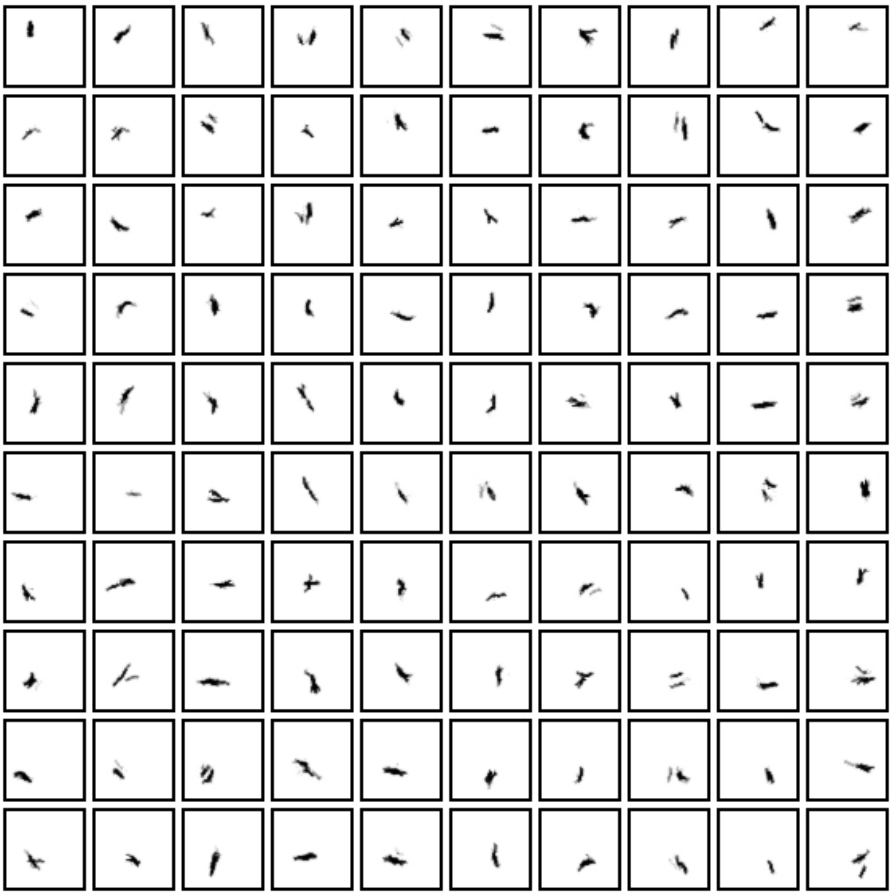

Figure 7: **The preferred stimuli of different V2 units.** The preferred patterns usually combine two different orientations, resulting in a corner, a junction, or a cross. There are also long lines formed by collinear edges of the same orientation, although they are less common. The patterns constitute the model's prediction of the preferred stimuli for orientation-selective V2 neurons.

and sizes, but in general the primary and secondary orientations together represent corner, junction, or cross in the visual field, depending on their relative locations.

This prediction is supported by the results of two independent studies in monkeys. First, discrete subregions within V2 receptive fields have been shown to prefer different orientations (Anzai & Van Essen, 2001, 2002; Anzai et al., 2002). This result suggests that the V2 neurons studied preferred more complicated patterns than straight lines: The model predicts that a combination of two different orientations constitutes such a preferred pattern.

Second, as described in the previous section, V2 neurons in macaque responded selectively to corners of different orientations and angles (Ito & Komatsu, 2004). This result is consistent with the preferred patterns of the model V2. Most of the corner-selective neurons in the empirical study also responded to a straight line with at least half of the response to the preferred corner. This result also agrees with the model, where the proportion of connection weights that represent the primary orientation is 0.6 ± 0.07.

6.2 Organization Within V2 Orientation Domain

An important observation on the model V2 is that within each orientation domain, there are units that have different secondary preferred orientations (Figure 6). These secondary orientations are shown systematically in Figure 5b. Throughout the map, units with the same secondary orientation preference form small clusters, or subdomains. Within a single orientation domain, there are usually several such clusters, suggesting that a substructure exists within the orientation domains.

Due to constraints on computation time and memory, the simulation had a limited resolution and it was not possible to study the substructure of the orientation domains further. However, based on the properties of the self-organizing model, it is likely that a larger simulation would result in many more subdomains than is visible in the current model. Further, they would be likely to be organized continuously into a secondary orientation map for each orientation domain. These predictions have not yet been studied in biology, but it can be verified with existing physiological techniques, e.g. by optical imaging.

7 Discussion

Using biologically grounded sizes for the receptive fields and lateral connections in the model, realistic orientation map and connectivity emerges in the model V1 through self-organization. Previous LISSOM-based models did not have such a direct correspondence of the sizes to their biological counterparts, making comparison and verification with experimental data difficult.

The model was extended to include V2, again imposing constraints from biological data. With the same principle of self-organization, an orientation map that matches physiological results developed: Orientation domains are larger in V2 and the changes of the preferred orientation are more abrupt (Hubel & Livingstone, 1987). The lateral connection patterns are patchy with individual patch size similar to V1, while the separation between the patches is larger in V2, matching biological data (Malach et al., 1994). The model V2 also has similar response statistics to the experimental data when different kinds of stimuli are presented (Hegdé & Van Essen, 2000, 2003; Ito & Komatsu, 2004). These results suggest that realistic connections in V2 can develop based on the same principles of self-organization as V1, providing a foundation for predicting other unknown but important properties of V2.

The main contribution of this paper is to provide two such verifiable predictions. First, most orientation-selective V2 receptive fields actually consist of two different orientations, thus forming selectivity of corners, junctions, or crosses. This prediction provides an explanation for the observations that some V2 receptive fields tune to different orientations (Anzai & Van Essen, 2001, 2002; Anzai et al., 2002), and that some V2 neurons are selective to both oriented lines and angles (Ito & Komatsu, 2004).

Second, the model predicts that each V2 orientation domain consists of subdomains of many different orientations. No direct evidence exists at this point for or against this idea: It is a prediction that arises from the self-organizing nature of the model. It can, however, be verified using current physiological techniques, e.g. optical imaging. The existence of different subdomains may also explain why the orientation domains are larger than those in V1, which is an open question at this point.

The prediction on the organization of orientation domains in V2 can also explain conflicting observations in the studies of feedback connections in V1 using tracers: In some studies, feedback from V2 was found to target V1 neurons of similar orientations (Shmuel et al., 2005; Angelucci, Schiessl, Nowak, & McLoughlin, 2003), while in another study no such preference was found (Stettler, Das, Bennett, & Gilbert, 2002). Because reciprocal connections are very common in the cortex, if the injection site of the tracer covers several subdomains, the tracer will show up in many domains of different orientations in V1. On the other hand,

if the injection site is located within a single subdomain, then a strong preference to the same orientation should be seen in V1.

Simple cells in V1 are crucial for shape processing, especially when the precise positions of the edges are important. The model V1 and the results presented in this paper are therefore based on simple cells only. However, V1 complex cells also project to V2 neurons. To determine how complex cells would affect the results, the simulation was repeated with simulated complex cells. A model V1 that contained only simple cells was first trained as in the original experiment to obtain the organization of orientation domains in V1. The receptive field of each unit was then replicated three times, with a $90^\circ, 180^\circ$, and 270° phase shift orthogonal to the preferred orientation of the unit. Each unit therefore had four receptive fields that preferred the same orientation, but at different phases. Complex cell response of a unit was then modeled using the energy model (Adelson & Bergen, 1985; D. Pollen & Ronner, 1983) by summing the square of the responses from each of the four receptive fields. The model V2 was trained using the complex cell response of V1. Interestingly, the results of V2 did not change: The preferred visual patterns still consisted of two different orientations, and there were different secondary orientation subdomains within orientation domains. The interpretation of the preferred patterns in V2 with complex cells as inputs is a little different from the simple-cell simulation, however, because the complex cell response is phase-invariant: $+$, $\top$, and L evoke similar responses in a V2 unit that prefers vertical and horizontal orientations. Nonetheless, this result shows that the predictions about V2 are robust and do not depend on the type of V1 cells that project to it.

One potential confound of the prediction about V2 receptive fields is that since V2 is smaller than V1, there may not be enough neurons in V2 to encode all the combinations of two different orientations. However, it may not be necessary to represent every combination of two orientations equally in the cortex. Combinations that occur rarely or are less useful for shape processing may be left out or encoded by fewer neurons. In fact, the results by Hegdé and Van Essen (2000, 2003) and Ito and Komatsu (2004) suggest that there are more V2 neurons that prefer small angles. Interestingly, as shown in the previous section, the model V2 also has the same preference, suggesting such biased representation originates from the statistics of natural images. Similarly, the orientations of the angles need not be represented equally, thus further reducing the number of neurons required. Note that even when combinations are absent or poorly represented in V2, they may still be accurately processed in higher visual areas. Many of these areas also have inputs from V1 that represents such orientations. Such filling-in may be one of the reasons why V1 projects to many high level areas directly (Felleman & Van Essen, 1991): commonly seen patterns are represented and processed more efficiently, while information of novel and rare patterns is still available to higher level areas that can process these patterns.

The model presented in this paper is simplified in the sense that it does not include feedback connections; such connections may also play a role in how receptive fields emerge during self-organization. In an extended version of LISSOM with feedback and smaller model V1 and V2 (Sit & Miikkulainen, 2006), V1 units formed receptive fields and an orientation map that were similar to those described in this paper. This result suggests that at least in lower visual areas, receptive fields can be driven mainly by a bottom-up process and may not be affected significantly by feedback connections. It is likely, however, that in higher areas the organization is more affected by what matters to the animal, and less by what exists in the visual environment. Such a change might be seen at the level of object representations although it is difficult to show at this point. However, combinations of self-organization and reinforcement learning have already been shown to be useful in robotic vision tasks (Chaput, 2004; Provost, Kuipers, & Miikkulainen, 2006).

8 Future Work

Because the receptive fields in the model are learned from the vast variety of structures contained in the natural input images, it is likely that they are general enough to be useful for shape processing. On the other hand, a shape is composed of several elements, and to perceive it as a whole, these elements have to be put together in some later stage in the brain. In particular, junctions and corners formed by two different orientation are crucial features for shape recognition (Biederman, 1987). It will therefore be useful to have neurons selective to them so that higher level areas can build more complicated receptive fields using these features as components. The prediction on the preferred patterns of V2 in this paper implies that such selectivity takes place in V2; how these patterns support shape processing in later stages of visual processing is an interesting direction for future work.

Since the focus of this paper is on receptive field properties for shape processing, other aspects like direction selectivity, ocular dominance, and color vision were not included in the model. The basic LISSOM model has recently been extended to show that a joint map of orientation, direction, and eye preference can be developed by self-organization in V1 (Bednar & Miikkulainen, 2006). In another extension, red and green photoreceptors have been included, and the model V1 self-organized to form realistic color and orientation maps (Bednar, De Paula, & Miikkulainen, 2005). By combining these two extensions with the current model, it may be possible to answer some interesting questions about V2. In particular, the thick, thin, and pale CO stripes, believed to process motion, color, and form, respectively, have an orderly organization in which the alternating thick and thin stripes are separated by pale stripes (Livingstone & Hubel, 1988; but see Sincich & Horton, 2005). How does such an organization develop in V2? Moreover, lateral connections in V2 are known to cross the stripes freely, thus linking neurons in different stripes (Levitt, Yoshioka, & Lund, 1994). Is there a general pattern of these connections and what is it? Most importantly, is there a reason for such a stripe organization and lateral connectivity in V2 for visual processing? Future studies using computational models like LISSOM can lead to insights that eventually allow answering these questions.

9 Conclusions

The receptive field properties for form perception in V2 are largely unknown, despite its size and proximity to V1 in the visual hierarchy. In this paper two predictions were developed, based on a computational model with realistic constraints: (1) Orientation-selective V2 cells prefer patterns that are formed by two edges of different orientations, such as a corner, junction, or cross; (2) Within each orientation domain in V2, there are subdomains that prefer different orientations. The first prediction is consistent with existing physiological results, while the second one novel; both predictions can be verified in animal studies with current techniques. These results demonstrate how computational models can be used to provide guidelines to experiments that may lead to a better understanding of the visual processing circuitry in the brain.

References

Adelson, E. H., & Bergen, J. R. (1985). Spatiotemporal energy models for the perception of motion. *Journal of the Optical Society of America A*, *2*, 284–299.

Amir, Y., Harel, M., & Malach, R. (1993). Cortical hierarchy reflected in the organization of intrinsic connections in macaque monkey visual cortex. *Journal of Comparative Neurology*, *334*, 19–46.

Angelucci, A., Levitt, J. B., Walton, E. J., Hupe, J. M., Bullier, J., & Lund, J. S. (2002). Circuits for local and global signal integration in primary visual cortex. *Journal of Neuroscience*, *22*, 8633–8646.

Angelucci, A., Schiessl, I., Nowak, L., & McLoughlin, N. (2003). Functional specificity of feedforward and feedback connections between primate V1 and V2. In *Society for neuroscience abstracts* (p. 911.9). Washington, DC: Society for Neuroscience.

Anzai, A., & Van Essen, D. C. (2001). Receptive field substructure of monkey V2 neurons in the orientation domain. In *Society for neuroscience abstracts* (p. 286.5). Washington, DC: Society for Neuroscience.

Anzai, A., & Van Essen, D. C. (2002). Receptive field structure of orientation selective cells in monkey V2. In *Society for neuroscience abstracts* (p. 720.12). Washington, DC: Society for Neuroscience.

Anzai, A., Van Essen, D. C., Peng, X., & Hegdé, J. (2002). Receptive field structure of monkey V2 neurons for encoding orientation contrast. *Journal of Vision*, *2*(7), 221a.

Bednar, J. A., De Paula, J. B., & Miikkulainen, R. (2005). Self-organization of color opponent receptive fields and laterally connected orientation maps. *Neurocomputing*, *65–66*, 69–76.

Bednar, J. A., & Miikkulainen, R. (2006). Joint maps for orientation, eye, and direction preference in a self-organizing model of V1. *Neurocomputing*, *69*(10–12), 1272–1276.

Biederman, I. (1987). Recognition-by-components: A theory of human image understanding. *Psychological Review*, *94*, 115–147.

Blasdel, G. G. (1992, August). Orientation selectivity, preference, and continuity in monkey striate cortex. *Journal of Neuroscience*, *12*, 3139–3161.

Bourgeois, J. P., Jastreboff, P. J., & Rakic, P. (1989). Synaptogenesis in visual cortex of normal and preterm monkeys: Evidence for intrinsic regulation of synaptic overproduction. *Proceedings of the National Academy of Sciences, USA*, *86*, 4297–4301.

Boynton, G. M., & Hegdé, J. (2004). Visual cortex: The continuing puzzle of area V2. *Current Biology*, *14*(13), R523–R524.

Burkhalter, A., & Van Essen, D. C. (1986). Processing of color, form and disparity information in visual areas VP and V2 of ventral extrastriate cortex in the macaque monkey. *Journal of Neuroscience*, *6*(8), 2327–2351.

Cai, D., DeAngelis, G. C., & Freeman, R. D. (1997). Spatiotemporal receptive field organization in the lateral geniculate nucleus of cats and kittens. *Journal of Neurophysiology*, *78*(2), 1045–1061.

Chaput, H. H. (2004). *The constructivist learning architecture: A model of cognitive development for robust autonomous robots*. Unpublished doctoral dissertation, Department of Computer Sciences, The University of Texas at Austin. (Technical Report TR-04-34)

DeAngelis, G. C., Ghose, G. M., Ohzawa, I., & Freeman, R. D. (1999). Functional micro-organization of primary visual cortex: Receptive field analysis of nearby neurons. *Journal of Neuroscience*, *19*(10), 4046–4064.

DeAngelis, G. C., Ohzawa, I., & Freeman, R. D. (1993, April). Spatiotemporal organization of simple-cell receptive fields in the cat's striate cortex. I. General characteristics and postnatal development. *Journal of Neurophysiology*, *69*(4), 1091–1117.

Deco, G., & Rolls, E. T. (2004). A neurodynamical cortical model of visual attention and invariant object recognition. *Vision Research*, *44*, 621–642.

Felleman, D. J., & Van Essen, D. C. (1991). Distributed hierarchical processing in primate cerebral cortex. *Cerebral Cortex*, *1*, 1–47.

Gattass, R., Gross, C. G., & Sandell, J. H. (1981). Visual topography of V2 in the macaque. *The Journal of Comparative Neurology*, *201*(4), 519–539.

Grossberg, S., & Williamson, J. R. (2001). A neural model of how horizontal and interlaminar connections of visual cortex develop into adult circuits that carry out perceptual grouping and learning. *Cerebral Cortex*, *11*, 37–58.

Hateren, J. H. van, & Schaaf, A. van der. (1998). Independent component filters of natural images compared with simple cells in primary visual cortex. *Proceedings of the Royal Society London B.*, *265*, 359–366.

Hayes, W. P., & Meyer, R. L. (1988a). Optic synapse number but not density is constrained during regeneration onto surgically halved tectum in goldfish: HRP-EM evidence that optic fibers compete for fixed numbers of postsynaptic sites on the tectum. *Journal of Computational Neurology*, *274*, 539–559.

Hayes, W. P., & Meyer, R. L. (1988b). Retinotopically inappropriate synapses of subnormal density formed by misdirected optic fibers in goldfish tectum. *Developmental Brain Research*, *38*, 304–312.

Hebb, D. O. (1949). *The organization of behavior: A neuropsychological theory*. Hoboken, NJ: Wiley.

Hegdé, J., & Van Essen, D. C. (2000). Selectivity for complex shapes in primate visual area V2. *Journal of Neuroscience*, *20*, RC61:1–6.

Hegdé, J., & Van Essen, D. C. (2003). Strategies of shape representation in macaque visual area V2. *Visual Neuroscience*, *20*, 313–328.

Hirsch, J. A., & Gilbert, C. D. (1991, June). Synaptic physiology of horizontal connections in the cat's visual cortex. *Journal of Neuroscience*, *11*, 1800–1809.

Hubel, D. H., & Livingstone, M. S. (1987). Segregation of form, color, and stereopsis in primate area 18. *Journal of Neuroscience*, *7*, 3378–3415.

Hubel, D. H., & Wiesel, T. N. (1959). Receptive fields of single neurons in the cat's striate cortex. *The Journal of Physiology*, *148*, 574–591.

Hubel, D. H., & Wiesel, T. N. (1962). Receptive fields, binocular interaction and functional architecture in the cat's visual cortex. *The Journal of Physiology*, *160*, 106–154.

Hubel, D. H., & Wiesel, T. N. (1965). Receptive fields and functional architecture in two nonstriate visual areas (18 and 19) of the cat. *Journal of Neurophysiology*, *28*, 229–289.

Ito, M., & Komatsu, H. (2004). Representation of angles embedded within contour stimuli in area V2 of macaque monkeys. *Journal of Neuroscience*, *24*(13), 3313–3324.

Jones, J. P., & Palmer, L. A. (1987). The two-dimensional spatial structure of simple receptive fields in cat striate cortex. *Journal of Neurophysiology*, *58*(6), 1187–1211.

Knierim, J. J., & van Essen, D. C. (1992). Neuronal responses to static texture patterns in area V1 of the alert macaque monkey. *Journal of Neurophysiology*, *67*, 961–980.

Levitt, J. B., Yoshioka, T., & Lund, J. S. (1994). Intrinsic cortical connections in macaque visual area V2: Evidence for interaction between different functional streams. *Journal of Comparative Neurology*, *342*, 551–570.

Liu, Z., Gaska, J. P., Jacobson, L. D., & Pollen, D. A. (1992). Interneuronal interaction between members of quadrature phase and antiphase pairs in the cats. *Vision Research*, *32*(7), 1193–1198.

Livingstone, M. S., & Hubel, D. H. (1984). Specificity of intrinsic connections in primate primary visual cortex. *Journal of Neuroscience*, *4*, 2830–2835.

Livingstone, M. S., & Hubel, D. H. (1988). Segregation of form, color, movement, and depth: Anatomy, physiology, and perception. *Science*, *240*, 740–749.

Lu, H. D., & Roe, A. W. (2007). Functional organization of color domains in V1 and V2 of macaque monkey revealed by optical imaging. *Cerebral Cortex*. (in press)

Mahon, L. E., & de Valois, R. L. (2001). Cartesian and non-cartesian responses in LGN, V1, and V2 cells. *Visual Neuroscience*, *18*, 973–981.

Malach, R., Amir, Y., Harel, M., & Grinvald, A. (1993). Relationship between intrinsic connections and functional architecture revealed by optical imaging and in vivo targeted biocytin injections in the primate striate cortex. *Proceedings of the National Academy of Sciences, USA*, *90*, 10469–10473.

Malach, R., Tootell, R. B. H., & Malonek, D. (1994). Relationship between orientation domains, cytochrome

oxidase stripes, and intrinsic horizontal connections in squirrel monkey area V2. *Cerebral Cortex*, *4*, 151–165.

Miikkulainen, R., Bednar, J. A., Choe, Y., & Sirosh, J. (2005). *Computational maps in the visual cortex*. Berlin: Springer.

Murray, M., Sharma, S., & Edwards, M. A. (1982). Target regulation of synaptic number in the compressed retinotectal projection of goldfish. *Journal of Computational Neurology*, *209*, 374–385.

Neumann, H., & Sepp, W. (1999). Recurrent V1-V2 interaction for early visual information processing. In M. Verleysen (Ed.), *Proceedings of the seventh european symposium on artificial neural networks ESANN 1999* (pp. 165–170).

Pallas, S. L., & Finlay, B. L. (1991). Compensation for population-size mismatches in the hamster retinotectal system: Alterations in the organization of retinal projections. *Visual Neuroscience*, *6*, 271–281.

Plebe, A. (2007). A model of angle selectivity development in visual area V2. *Neurocomputing*, *70*(10–12), 2060–2063.

Pollen, D., & Ronner, S. (1983). Visual cortical neurons as localized spatial frequency filters. *IEEE Trans. on Systems, Man, and Cybernetics*, *13*, 907–916.

Pollen, D. A., & Ronner, S. F. (1981). Phase relationships between adjacent simple cells in the visual cortex. *Science*, *212*(4501), 1409–1411.

Provost, J., Kuipers, B. J., & Miikkulainen, R. (2006). Developing navigation behavior through self-organizing distinctive state abstraction. *Connection Science*, *18*(2).

Purves, D. (1988). *Body and brain: A trophic theory of neural connections*. Cambridge, MA: Harvard University Press.

Purves, D., & Lichtman, J. W. (1985). *Principles of neural development*. Sunderland, MA: Sinauer.

Ringach, D. L. (2004). Mapping receptive fields in primary visual cortex. *The Journal of Physiology*, *558*, 717–728.

Rodieck, R. W. (1965). Quantitative analysis of cat retinal ganglion cell response to visual stimuli. *Vision Research*, *5*(11), 583–601.

Ross, W. D., Grossberg, S., & Mingolla, E. (2000). Visual cortical mechanisms of perceptual grouping: Interacting layers, networks, columns, and maps. *Neural Networks*, *13*, 571–588.

Sceniak, M. P., Hawken, M. J., & Shapley, R. (2001). Visual spatial characterization of macaque V1 neurons. *Journal of Neurophysiology*, *85*(5), 1873–1887.

Schwartz, O., Pillow, J. W., Rust, N. C., & Simoncelli, E. P. (2006). Spike-triggered neural characterization. *Journal of Vision*, *6*(4), 484–507.

Shmuel, A., Korman, M., Sterkin, A., Harel, M., Ullman, S., Malach, R., et al. (2005). Retinotopic axis specificity and selective clustering of feedback projections from V2 to V1 in the owl monkey. *Journal of Neuroscience*, *25*(8), 2117–2131.

Sincich, L. C., & Horton, J. C. (2005). The circuitry of V1 and V2: integration of color, form, and motion. *Annual Review of Neuroscience*, *28*, 303–326.

Sirosh, J., & Miikkulainen, R. (1994). Cooperative self-organization of afferent and lateral connections in cortical maps. *Biological Cybernetics*, *71*, 66–78.

Sit, Y. F., & Miikkulainen, R. (2006). Self-organization of hierarchical visual maps with feedback connections. *Neurocomputing*, *69*(10–12), 1309–1312.

Stettler, D. D., Das, A., Bennett, J., & Gilbert, C. D. (2002). Lateral connectivity and contextual interactions in macaque primary visual cortex. *Neuron*, *36*(4), 739–750.

Sullivan, T. J., & de Sa, V. R. (2006). A model of surround suppression through cortical feedback. *Neural Networks*, *19*(5), 564–572.

Tavazoie, S. F., & Reid, R. C. (2000). Diverse receptive fields in the lateral geniculate nucleus during thalamocortical development. *Nature Neuroscience*, *3*(6), 608–616.

Taylor, N. R., Hartley, M., & Taylor, J. G. (2005). Coding of objects in low-level visual cortical areas. In W. Duch, J. Kacprzyk, E. Oja, & S. Zadrozny (Eds.), *Proceedings of the 15th international conference on artificial neural networks ICANN 2005* (pp. 57–63). Berlin: Springer.

Turrigiano, G. G. (1999). Homeostatic plasticity in neuronal networks: The more things change, the more they stay the same. *Trends in Neurosciences*, *22*(5), 221–227.

Weliky, M., Kandler, K., Fitzpatrick, D., & Katz, L. C. (1995, September). Patterns of excitation and inhibition evoked by horizontal connections in visual cortex share a common relationship to orientation columns. *Neuron*, *15*, 541–552.

Weller, R. E., & Kaas, J. H. (1983, Novemember). Retinotopic patterns of connections of area 17 with visual areas V-II and MT in macaque monkeys. *The Journal of Comparative Neurology*, *220*(3), 253–279.

Zhaoping, L. (2005). Border ownership from intracortical interactions in visual area V2. *Neuron*, *47*, 143–153.

Zhou, H., Friedman, H. S., & von der Heydt, R. (2000). Coding of border ownership in monkey visual cortex. *Journal of Neuroscience*, *20*(17), 6594–6611.